Materials Research. 2023; 26:e20220325
DOI: https://doi.org/10.1590/1980-5373-MR-2022-0325

Experimental Investigation on the Effect of Stacking Sequence on Damage Resistance and Post-indentation Performance of Glass/Epoxy Laminates Under Different Loading Planes Using Acoustic Emission Monitoring

A. Usha Bharathi[a*], *V. Arumugam*[b], *C. Suresh Kumar*[c]

[a]*Jeppiaar Engineering College, Department of Aeronautical Engineering, Old Mamallapuram Road, Semmenchery, Chennai-119, Tamil Nadu, India.*
[b]*Anna University, Madras Institute of Technology Campus, Chromepet, Department of Aerospace Engineering, Chennai-44, Tamil Nadu, India.*
[c]*Bharath Institute of Higher Education and Research, Department of Aeronautical Engineering, Selaiyur, Chennai-73, Tamil Nadu, India.*

Received: July 19, 2022; Revised: October 25, 2022; Accepted: November 22, 2022

This research work focuses on the experimental investigation of indentation damage resistance and post-indented performance of different stacking sequence of glass/epoxy laminates using mechanical and acoustic responses. The laminates with stacking sequence, namely $[0]_{12}$, $[0/90]_{6S}$, $[+45/-45]_{6S}$ and $[0/+45/-45/90]_{3S}$ were subjected to normal and inclined indentation with acoustic emission monitoring. Quasi-static indentation (QSI) test was conducted on the center of the laminates using a hemispherical steel indenter with 12.7 mm diameter. The residual strength of the laminates was computed by conducting flexural after indentation test. Mechanical responses such as peak force, residual dent, linear stiffness and absorbed energy were employed to assess induced damages. The results reveal that the quasi-isotropic (QIS) laminates having better indentation damage resistance under 0^o and 10^o loading planes, whereas the angle-ply (AP) laminates performed well at 20^o. Moreover, the normalised cumulative counts, energy rate, peak frequency, AE hits and sentry function were used to evaluate the damage initiation and propagation. Further, AE results show that the shear induced damage has been reduced in AP as compared with QIS laminates under 20^o indentation plane. Finally, this study concluded that the QIS and AP laminates exhibited better indentation resistance under 0^o and 10^o, and 20^o loading planes respectively.

Keywords: *Indentation damage, Acoustic emission, Peak frequency, Sentry function, Residual flexural strength.*

1. Introduction

Fiber reinforced polymer (FRP) composite materials are extensively replacing the conventional metallic materials in many fields such as aerospace, marine and automotive industry due to higher specific strength, stiffness, dimensional stability, better corrosion resistance, long-term durability and excellent fatigue properties. However, the main limitation of composite materials is susceptibility to impact induced damage[1,2]. Many researchers have investigated the effect of matrix, fiber/matrix interfacial bonding and fiber properties of composite laminates for improving impact and residual strength[3,4]. Sohn et al.[5] and Bull et al.[6] have reported that the barely visible impact damage (BVID) is induced on the aircraft structures during pre-flight and taxiing operations, by runway debris, hail and bird strikes. This type of impact damage was simulated by conducting quasi-static indentation (QSI) loading on the composite structures[7]. Moreover, Yuichiro et al.[8] stated that the significant reduction of structural strength in laminated composites is mainly due to the severity of impact induced damage; it may be invisible during routine visual inspection methods[9].

The damage occurred during drop weight impact on the composite laminates was found similar behaviour under indentation loading[10,11]. Zhong et al.[12] and He et al.[13] proved that the quasi-static indentation (QSI) test can be used for simulating the impact events because the absorbed energy and damage morphology are equivalent for both tests. The indentation response was studied using mechanical parameters such as energy absorption, residual deformation and peak loads in each cycle of indentation loading[14-16]. Caprino et al.[17] concluded that the indentation induced damage was varied with respect to fiber orientation and configuration of glass/aluminum hybrid laminates. Jac Fredo et al.[18] quantified the global and local damages in glass/epoxy laminates using geometrical features which were extracted from the acquired digital images on the indented sites. Further, they have developed a model to detect the indentation induced damages in glass/epoxy composite laminates[19]. The effect of induced damage on the structure has perceived by the size/area of the damage during indentation loading. If the damage is not visible (the

* e-mail: ushabharathi.mit@gmail.com

induced damage is less than BVID), then the composite structures can withstand high ultimate load. On the other side, if the damage is visible (the induced damage is more than BVID), another decisive factor must be considered, like repair[20] or replace with new structural components[21].

Many researchers have focused on compression after impact (CAI) properties because the impact induced damage causes faster growth of delamination propagation under in-plane loading[3]. However, very few studies were carried out on the residual flexural properties because the flexural load evolves a complex stress pattern and their test parameter is harder to analyze[22,23]. Further, the composite structures have been subjected to all kinds of out-of-plane loading during service such as airfoil, bulkheads section etc. This leads to the importance of research on flexural properties of the composite laminates. However, nondestructive testing (NDT) methods have been widely used for the analysis of damage evolution in FRP composites under out-of-plane loading[24]. Acoustic emission (AE) is an effective NDT method for monitoring damage evolution in laminated composites[25-28]. AE signal is the phenomenon of transient elastic strain waves generated inside the materials when it undergoes deformation or fracture. Therefore, this technique is capable to detect *in-situ* information about damage mechanisms in the laminated composites under in-service operation.

Kumar et al.[29] discriminated the failure modes in laminated composites using AE amplitude, rise time, counts, energy, duration and peak frequency. Moreover, Mei et al.[30] used AE energy for investigating the fracture toughness[31,32] and failure strength prediction in polymer[33] and ceramic matrix[34] composites. They concluded that the residual strength of composites was associated with fiber bundles buckling and delamination[35]. However, a comprehensive damage characterization was made by correlating acoustic energy and mechanical strain energy for investigating the damage resistance in laminated composites[3,36]. This method was employed to evaluate the damage progression and residual strength of composite laminates under out-of-plane loading[1,37]. In fact, the aircraft structure has subjected to impact/indentation need not be normal to the plane of the structural elements. Normal indentation can causes maximum damage in the isotropic and homogenous materials. This statement has taken to be true by some researcher and industry expert.

To overcome the aforementioned gap in literature, it is necessary to carry out a research on the effect of different angles of impact/indentation on the structural elements with efficient AE based method to characterize the damage resistance and post-indentation performance of glass/epoxy laminates under normal and inclined planes of loading. In this study, the effect of stacking sequence of glass/epoxy composite laminates on indentation damage resistance and its residual strength were investigated. The stacking sequence such as $[0]_{12}$, $[0/90]_{6S}$, $[+45/-45]_{6S}$ and $[0/+45/-45/90]_{3S}$ were subjected to 4 mm indentation displacement under normal (0^o) and inclined (10^o and 20^o) planes of loading with acoustic emission (AE) monitoring. The correlation between mechanical and AE results were performed to quantify the extent of indentation induced damage. Further, the post-indented performance of laminates was estimated by conducting three point bending tests.

2. Experimental procedures

2.1. Materials and fabrications

A stitch-bonded unidirectional glass fiber with a mass density of 220 g/m^2 was used as reinforcement for the fabrication of the composite laminates. Epoxy resin (LY556) with hardener (HY 951) in the ratio of 10:1 was used as the matrix material. Twelve layers of glass fabrics with stacking sequence, namely $[0]_{12}$ unidirectional (UD), $[0/90]_{6S}$ cross-ply (CP), $[+45/-45]_{6S}$ angle-ply (AP) and $[0/+45/-45/90]_{3S}$ quasi-isotropic (QIS) were fabricated using hand layup process. The laminates were allowed to cure using a 50 kN compression molding machine at a hydraulic pressure of 50 kg/cm^2 and room temperature for 24 hours. Care was taken to maintain the same thickness for all laminates. ASTM D790-10 standard flexural test specimen sizes of 150 x 40 mm were cut from the fabricated laminate thickness of 3.5 (±0.15) mm using a water jet cutting machine.

2.2. Indentation test

Quasi-static indentation (QSI) test was conducted using a Tinius Olsen Universal Testing Machine (UTM) as shown in Figure 1. Specimens were clamped on the base plate with a central circular hole diameter of 30 mm on the QSI fixture. The indentation loading were applied at the center of the specimens under normal (0^o) and inclined (10^o and 20^o) planes. The damage was induced by using hemispherical steel indenter of diameter 12.7 mm with a velocity of 1 mm/min. The damage resistance on the specimens was measured upto 4 mm transverse displacement of indenter. The parameters such as peak force, residual dent and absorbed energy were used for evaluating the indentation resistance. Five specimens were tested in each case for calculating the average values.

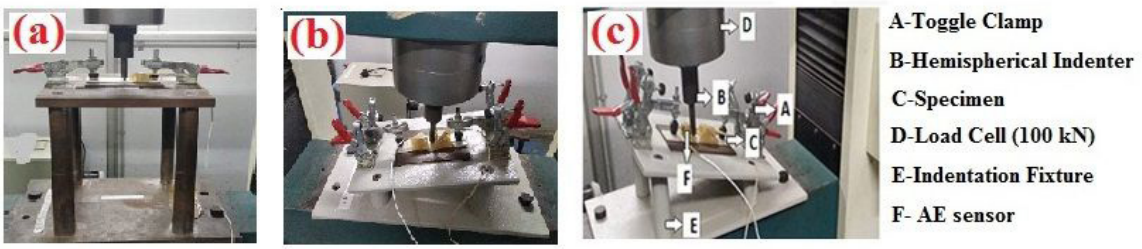

Figure 1. QSI test fixture for different loading planes (a) 0^o, (b) 10^o and (c) 20^o.

2.3. Flexural after indentation (FAI) tests

Three point bending test was carried out on the post-indented glass/epoxy laminates for estimating the residual flexural strength using Tinius Olsen UTM. The transverse load was applied at a constant cross head speed of 0.5 mm/min as shown in Figure 2. The span was kept as 100 mm. This test was conducted for evaluating the intensity of indentation induced damage on the different stacking sequence of glass/epoxy laminates under normal (0^o) and inclined (10^o) planes of loading.

2.4. Acoustic emission (AE) monitoring

Quasi-static indentation (QSI) and flexural after indentation (FAI) tests were conducted individually using Tinius Olsen UTM with online AE monitoring. An eight channel AE system supplied by Physical Acoustic Corporation (PAC) (Princeton, NJ, USA) with a sampling rate of 3 MHz and a 40 dB pre-amplification was used for this investigation. Ambient noise was filtered using a threshold of 45 dB. However, AE measurement was performed during QSI test using two wide band (WD) sensors in a linear arrangement. The nominal distance between the two sensors was kept as 100 mm. AE sensors were placed on the specimen surface using high vacuum silicon grease. A typical pencil lead break test was conducted for generating repeatable AE signals for the calibration of each sensor, wave propagation and factors like attenuation loss were taken into account. The average wave velocity was found to be in the range 3000 m/s and the timing parameters were fixed according to the wave velocity obtained. The peak definition time (PDT) was determined as 31 µs, hit definition time (HDT) and hit lock out time (HLT) were set to 300 µs and 600 µs respectively.

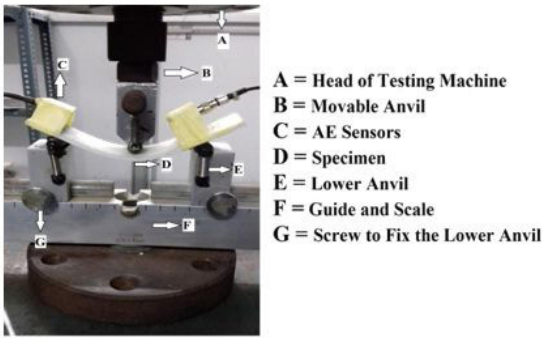

Figure 2. Experimental setup for three point bending test.

3. Results and Discussion

In this study, the effect of stacking sequence of glass/epoxy laminates under normal (0^o) and inclined (10^o and 20^o) planes of indentation loading and post-indentation performance of laminates were investigated using mechanical and acoustic responses. The results are summarized as follows.

3.1. Mechanical results

The glass/epoxy laminates with different stacking sequence such as unidirectional (UD), cross-ply (CP), angle-ply (AP), and quasi-isotropic (QIS) composites were subjected to normal (0^o) and inclined (10^o and 20^o) planes of quasi-static indentation (QSI) loading to evaluate impact induced damage resistance. The peak force versus indentation displacement of the laminates is shown in Figure 3. The QIS glass/epoxy laminates exhibited the highest contact force followed by AP, CP and UD laminates. Similar trends were observed in all loading planes. In the case of 10^o and 20^o loading plane, the significant reduction of peak force was noticed as compared with normal plane. This might be due to less contact between the specimen surface and indenter by increasing the angle

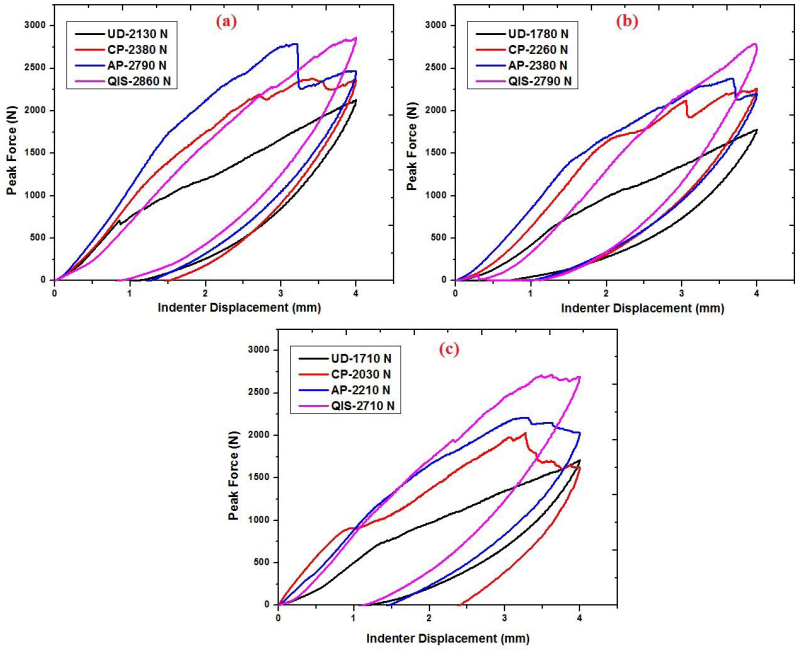

Figure 3. Indentation displacement Vs Peak force under different indentation loading planes (a) 0^o, (b) 10^o and (c) 20^o.

of loading plane. On the other hand, the reduction of peak force is due to the distribution of inclined indented force along x-component (shear) and y-component (normal). However, the angle of loading plane is increases; there is a rise in x-component force and fall in y-component force. Hence, the 20° indentation loading plane shows constant peak force at higher indentation displacement between 3 to 4 mm which reveals the shear failure of delamination and fiber/matrix interfacial debonding might be occurred for all cases of laminates.

Based on the materials response, the sudden drop of peak force was reduced in the case of AP laminates. Therefore, AP laminates have a better resistance to shear failure with increase the angle of indentation loading. Conversely, CP laminates have susceptible to indentation induced damage such as fiber/matrix interfacial debonding and delamination with increase the angle of loading plane. However, the slight reduction of peak force in UD laminates was occurred due to fiber/matrix interfacial debonding. In all stacking sequence, the QIS laminates produced better indentation damage resistance under normal and inclined loading planes. Further, it is evident that the residual dent of UD, CP, AP and QIS laminates under 10° loading plane, which was reduced by 36.73%, 34.44%, 19.84% and 49.66% respectively as compared with normal indentation. In the case of 20° indentation plane, the residual dent of UD, CP, AP and QIS laminates was increased by 12.93%, 90.91%, 20.71% and 49.52% respectively as compared with 0° indentation loading. Moreover, QIS laminates offered more resistance to induce permanent dent followed by AP, CP and UD laminates under 0°, 10° and 20° indentation loading planes as shown in Figure 4a.

The linear stiffness of different stacking sequence of glass/epoxy laminates was computed by the slope between the peak force and indenter displacement before the first drop of load. The linear stiffness of all cases of laminates is shown in Figure 4b. In the case of 0° indentation plane, all laminates exhibited higher linear stiffness due to more contact force as compared with inclined plane of loading. Further, the laminates indented at 10° indicated the reduction of linear stiffness by 30.59%, 21.08%, 19.07% and 5.44% when compared with normal indentation for UD, CP, AP and QIS respectively. Besides, 20° indented UD and AP laminates shown a decrease in stiffness as 17.32% and 12.91% whereas the stiffness was increased by 3.66% and 4.46% for CP and QIS laminates respectively.

The peak force and incident energy are directly proportional to the linear stiffness and local bending resistance of the laminates. It is shown in Figure 5a and b. In normal loading plane, the peak force is higher for AP and QIS laminates whereas in 10° and 20°, the QIS laminates exhibited better load bearing capacity as compared with AP. However, the total energy imposed on AP laminates is more than the QIS laminates under normal and inclined loading planes. This might be due to better rigidity modulus and shear damage resistance in AP laminates. The absorbed energy and elastic energy are the significant parameters to measure the extent of indentation induced damage which is depicted in Figure 5c and d. The elastic energy was decreased from 0° to 10° indentation loading for UD, AP and QIS laminates but it was increased by 4.69% for CP laminates. Moreover, the absorbed energy is decreased for all cases of laminates under the loading from 0° to 10° and reverse trends were observed from 10° to 20° loading plane due to the distribution of indentation force along x-components (shear) and y-components (normal) which was evidenced by the residual dents.

3.2. Analysis of AE activities during indentation

The indentation damage resistance in different stacking sequences of glass/epoxy laminates is analysed using the significant AE parameters such as peak frequency, normalized cumulative counts (NCC) and energy rate under normal and inclined planes of loading as shown in Figures 6 and 7. Based on the damage evolution, three different slopes have been obtained in the NCC and the corresponding three different values of AE energy rate are < 0.2aJ, ≈ 0.5aJ and > 0.5aJ. The lowest slope of NCC with low value of 0.2 aJ indicates the initiation of micro damage and it does not have a significant reduction of stiffness. The macro damage was occurred in the greatest slope of NCC with medium value

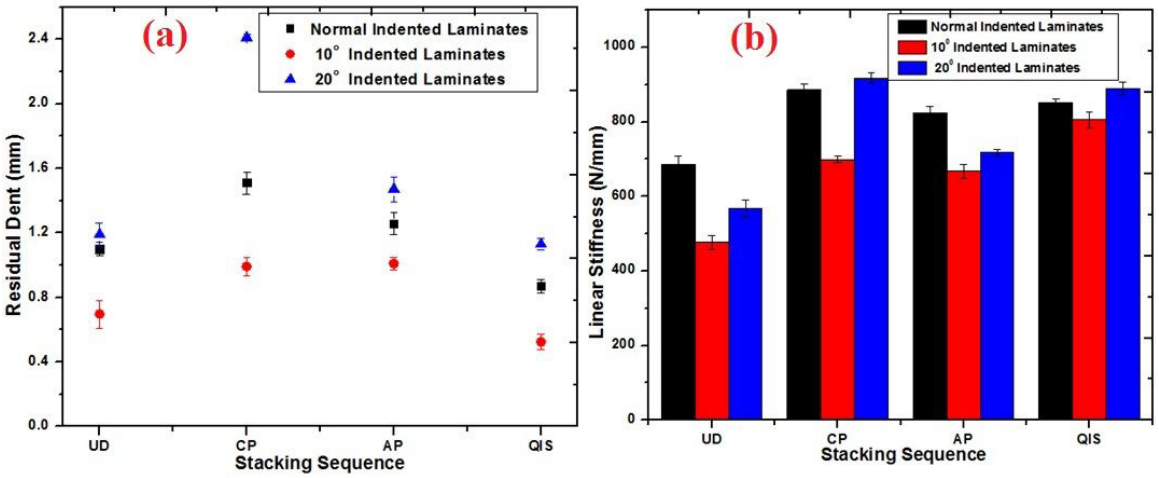

Figure 4. Evaluation of damage resistance (a) Residual dent and (b) Linear stiffness.

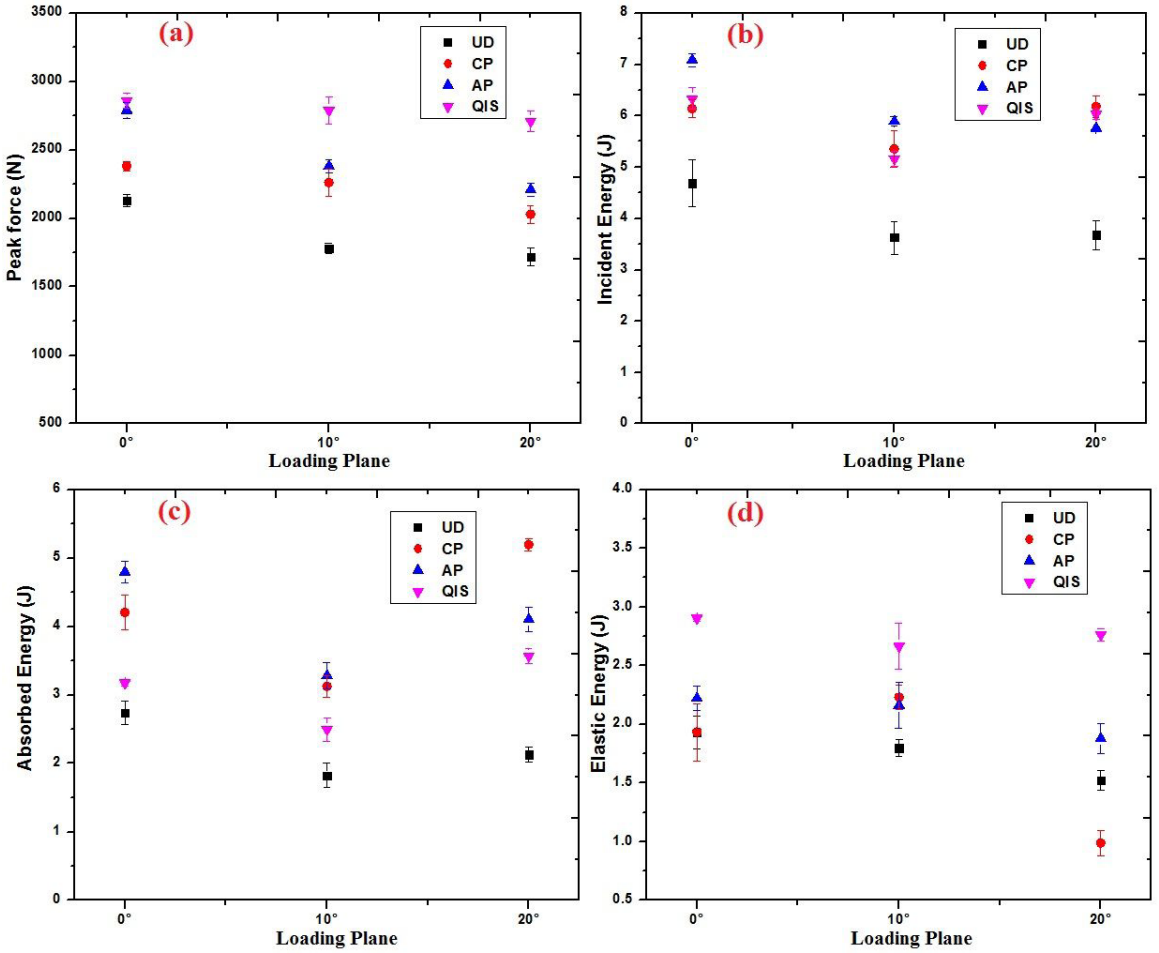

Figure 5. Effect of stacking sequence of glass/epoxy laminates on different loading planes (a) Peak force, (b) Incident Energy, (c) Absorbed Energy and (d) Elastic Energy.

of ≈ 0.5aJ. However, the biggest slope of NCC with a high value of > 0.5aJ leads to the catastrophic failure. A few hits with energy rate nearer to zero are associated with friction between crack faces or irregular stress relief.

The extent of damage is more in UD, CP and AP laminates under normal indentation as compared with inclined plane as shown in Figures 6 and 7. But, the reverse trend was observed in AP laminates. Therefore, very less AE hits were detected related to each damage modes in AP and QIS laminates under 20° and 0° loading planes respectively. Moreover, AE result shows better indentation damage resistance in AP and QIS laminates. The damage modes such as matrix cracking, delamination, fiber/matrix interfacial debonding and fiber failure were observed in all cases of laminates under 0°, 10° and 20° indentation loading. Further, AE signals analysis was performed for all stacking sequences of laminates to identify the frequency ranges of each damage modes. The damage progression and their distinct frequency range of each damage modes in CP laminates are shown in Figures 6 and 7. The peak frequency range of 60 - 120 kHz is indicated as matrix cracking. Similarly, the frequency ranges of 130 - 180 kHz, 190 - 260 kHz and 270 - 320 kHz are represented as delamination, fiber/matrix interfacial debonding and fiber failure respectively during the indentation process of laminates[24,25].

The percentage of AE hits related to each damage modes in all laminates is shown in Figure 8. Matrix cracking is occurred at an earlier stage of loading and dominated throughout the process of indentation. Therefore, the percentage of AE hits related to matrix cracking is high for all stacking sequences and loading planes which are depicted in Fig.8. Furthermore, the shear failure of fiber/matrix interfacial debonding and delamination were progressed under inclined indentation loading plane. However, the shear induced damage of fiber/matrix interfacial debonding and delamination were reduced in AP laminates as compared with QIS laminates under 20° indentation loading. This might be due to high damage tolerance and shear resistance in AP laminates. Thus, the percentage of AE hits related to fiber/matrix interfacial debonding and delamination in AP is lesser than QIS followed by CP and UD laminates. Moreover, the percentage of AE hits related to fiber failure is reduced as increase the angle of indentation loading up to 45°. Nevertheless, the AP and QIS laminates showed better damage resistance under inclined indentation loading.

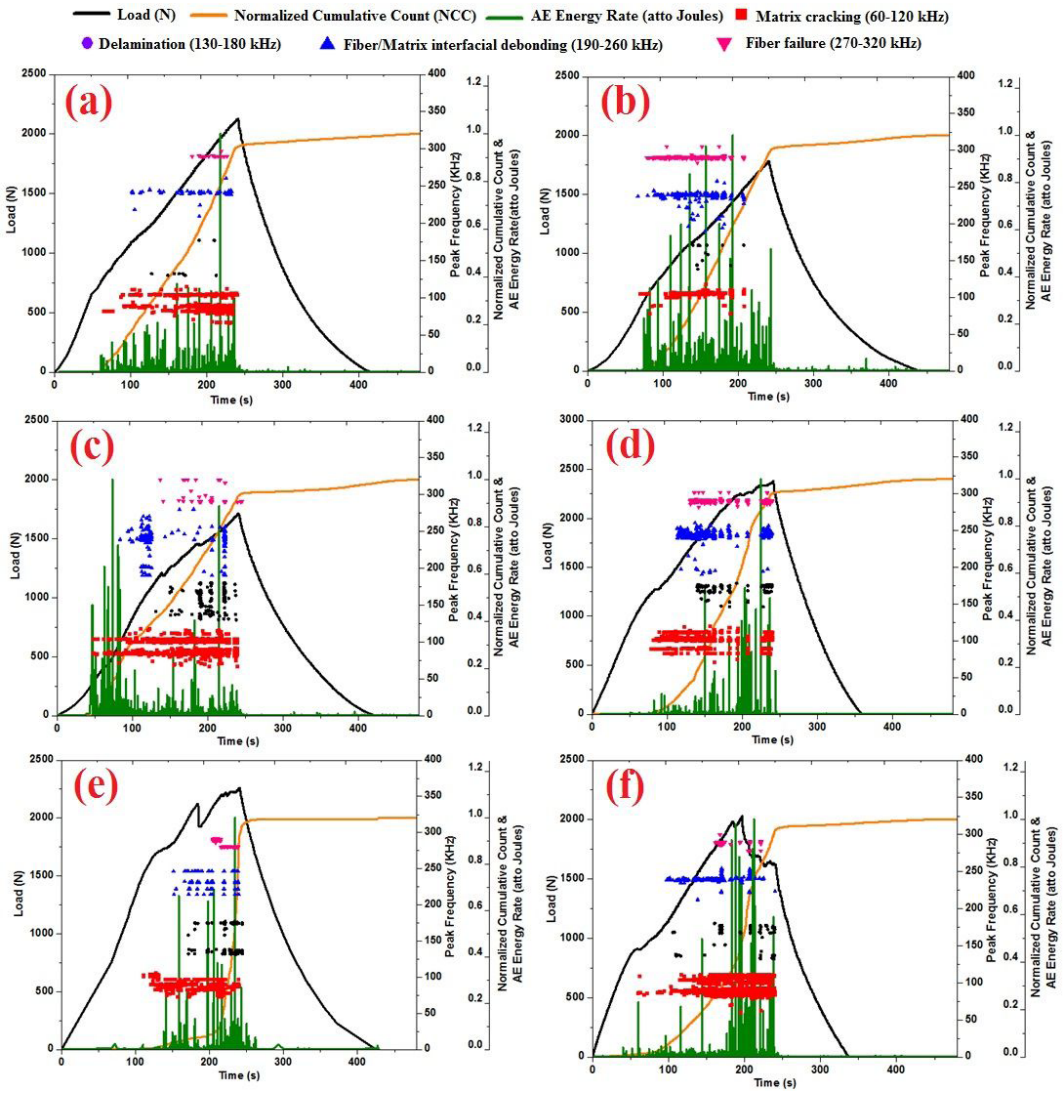

Figure 6. Representation of AE activities during indentation: (a) UD@0º, (b) UD@10º, (c) UD@20º, (d) CP@0º, (e) CP@10º and (d) CP@20º.

3.3. Damage evaluation using sentry function

Sentry function is defined as the natural logarithm of the ratio between the mechanical strain energy and acoustical energy[38]. It is represented in Equation 1

$$f(x) = Ln\left[\frac{E_S(x)}{E_a(x)}\right] \quad (1)$$

where x is the displacement, E_s is the mechanical strain energy and E_a is the AE energy. This function correlates the mechanical strain energy and AE energy which can provides intensive analysis of damage propagation in laminated composites[39]. It has four distinct phases of P_I, P_{II}, P_{III} and P_{IV}.

(a). P_I – This phase related to increase of strain energy. During the initial stage of loading, the sentry function is increased due to accumulation of mechanical strain energy and negligible AE energy. Thus, the damage occurs in the laminates is insignificant.

(b). P_{II} – This phase related to sudden drop of sentry function due to instantaneous increase of AE energy and low strain energy. This indicates the reduction of stiffness and initiation of macroscopic damage in the laminates.

(c). P_{III} – This phase denoted the constant trend of sentry function by the equilibrium state of mechanical strain energy and AE energy.

(d). P_{IV} – This phase represented the gradual decrease of sentry function due to the propagation of damage growth and degradation of laminates.

Based on the description of various trends of sentry function, the small fall of P_{II} function indicates the initiation of micro damage and the big fall of P_{II} function shows the occurrence of macro damage. The significant internal damage in the laminate exhibited sudden release

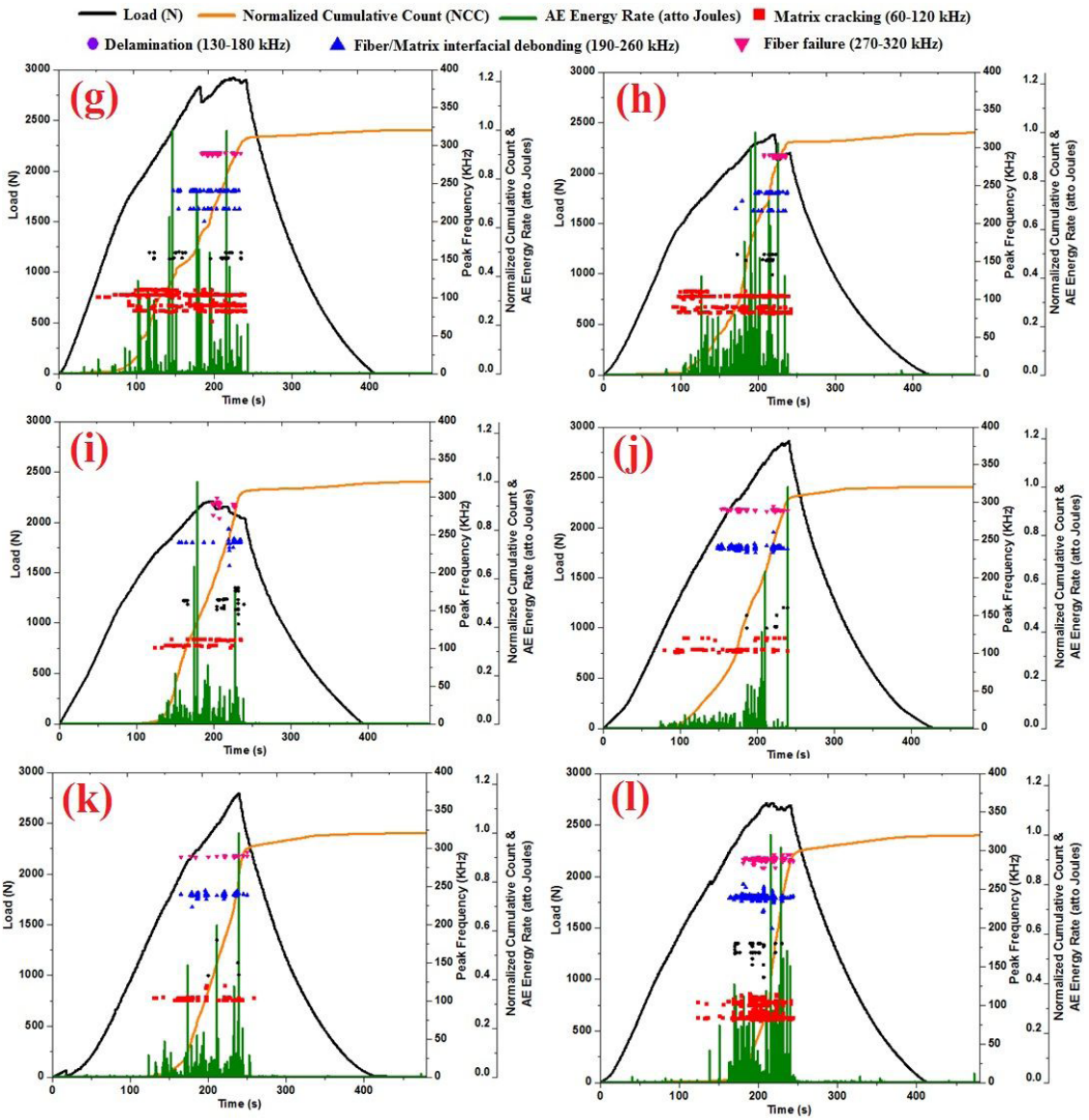

Figure 7. Representation of AE activities during indentation: (g) AP@0°, (h) AP@10°, (i) AP@20°, (j) QIS@0°, (k) QIS@10° and (l) QIS@20°.

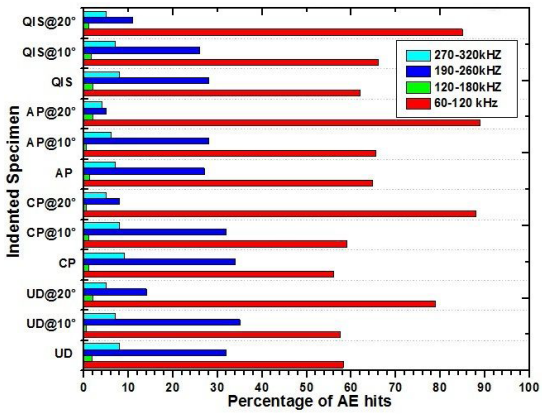

Figure 8. Percentage of AE hits for each damage modes.

of stored strain energy which can be recorded as a high energy content of AE signal. Figure 9 shows the effect of stacking sequence of glass/epoxy laminates under different loading plane during indentation process. The big fall of P_{II} function was observed in UD laminates under normal indentation loading. When increasing the loading plane from 0° to 20°, the length of the big fall of P_{II} function has been reduced. This reveals that the severity of damage is more at 0° and 10° loading planes. Further, the evidence was obtained from the residual dent and absorbed energy. However, the UD laminates offered better resistance to indentation damage at 20° loading plane. In contrast, the catastrophic failure was observed in CP laminates at 20° indentation loading. Two big fall of P_{II} was found in CP laminates at 20° loading plane. This reveals the degradation of structural integrity and propagation of damage growth

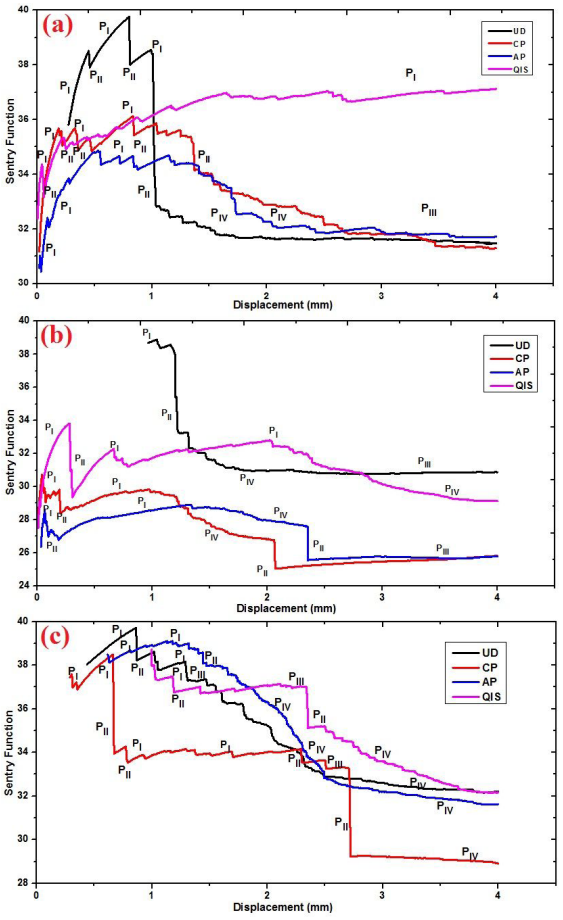

Figure 9. Damage evaluation in glass/epoxy laminates under different loading planes (a) 0°, (b) 10° and (c) 20°.

were occurred. This is shown in photographic images of indented laminates in Figure10. However, more number of P_I function and less number P_{II} function of CP laminates produced better indentation damage resistance under normal (0°) indentation loading as compared with 10° and 20°.

In the case of QIS laminates, there is no P_{II} function and more number of P_I function were found. Moreover, P_I and P_{III} functions could be seen at the higher indentation displacement under normal (0°) indentation loading. Further, big fall of P_{II} function was obtained at 10° and 20° indentation loading. In addition that three P_I and one P_{III} function were found in QIS laminates under 10° loading plane. Therefore, QIS laminates exhibited better indentation resistance at 0° and 10° loading planes. However, the damage propagation is very sensitive beyond 2.3 mm indentation displacement in QIS laminates under 20° loading plane. This is evidenced from the residual dent, absorbed energy and photographic images of indented laminates. Similarly, for the case of AP laminates, more number of P_I, P_{III} and P_{IV} functions was observed under 20° loading plane. Additionally, small P_{II} function could be appeared in AP laminates under 0° and 10° loading planes. Finally, the AP laminates show better indentation damage resistance under 20° loading plane. This might be due to better shear induced damage resistance in AP laminates. Nonetheless, this study concluded that the QIS laminates can be used for low indentation angle between 0° and 10°, whereas the AP can be used for high indentation angle between 20° and 45° to offer better resistance to indentation damages.

3.4. Estimation of residual flexural strength

The indented and non-intended laminates were subjected to flexural test to investigate the effect of stacking sequence and indentation angle on the computation of residual flexural strength. Figure 11a shows the flexural strength

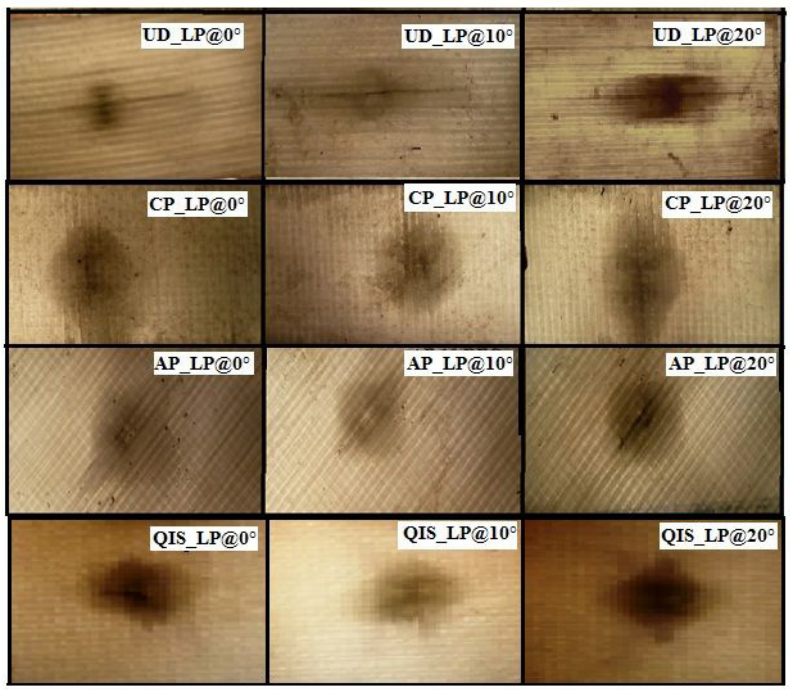

Figure 10. Rear side photographic view of indented glass/epoxy laminates under different loading planes (LP).

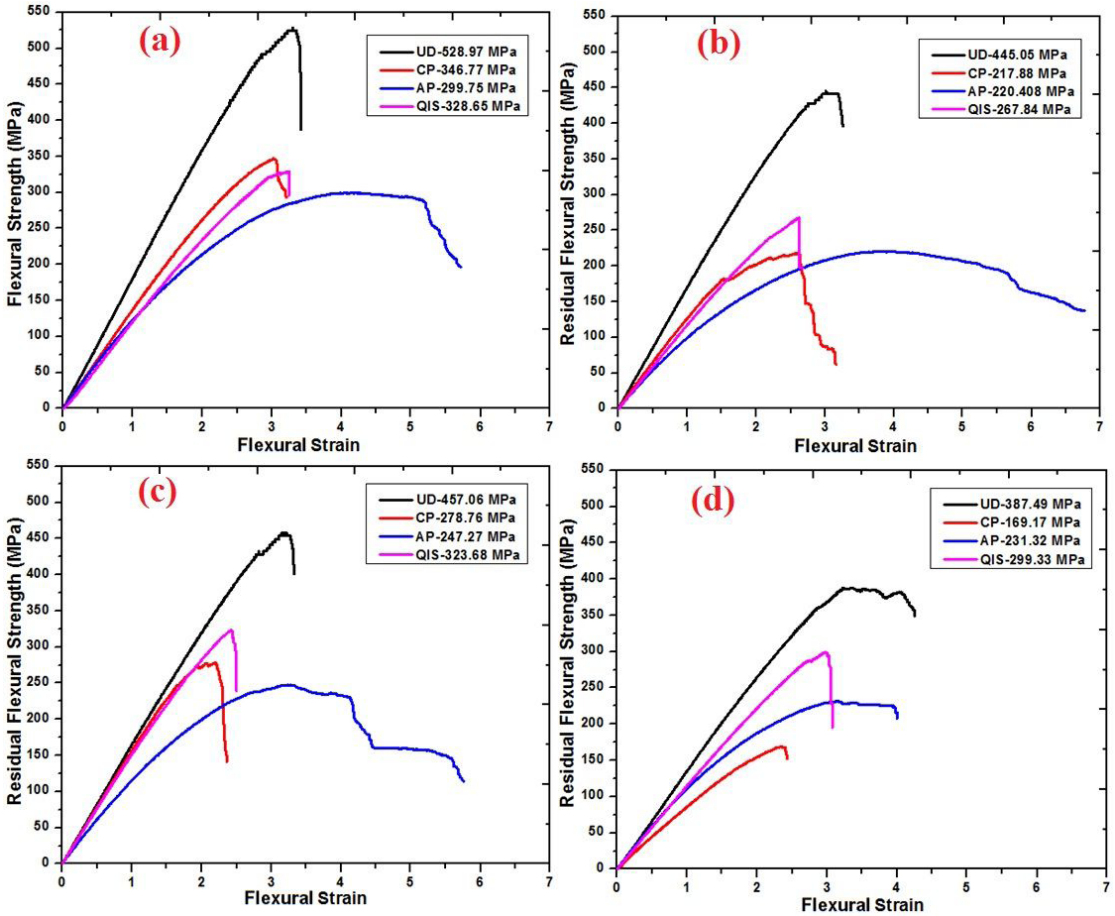

Figure 11. Estimation of residual flexural strength (a) Non-indented, (b) Indented at 0°, (c) Indented at 10° and (d) Indented at 20°.

of non-indented laminates. The result reveals that the UD laminates exhibited highest flexural strength followed by CP, QIS and AP laminates. This might be due to the longitudinal direction of fibers being able to carry more loads. Further, the bending stiffness of UD is higher than CP, QIS and AP laminates. However, the residual flexural strength has been reduced with increase the angle of indentation loading for all cases of laminates. This is evidence of the fact that the laminates have highest residual dent and absorbed energy. In all cases of indentation loading planes, the strain to failure rate was observed as high for AP laminates. The residual flexural strength of QIS laminates is quit higher than CP and AP laminates. This showed that QIS laminates causes significantly less fiber/matrix interfacial debonding and delamination as compared with CP and AP laminates under 0° and 10° indentation loading. Conversely, the AP laminates performed better residual strength at 20° indentation loading as compared with 0° and 10° which is indicated in Figure 11b-d.

The percentage reduction of residual flexural strength is shown in Figure 12. At 10° indentation loading, the laminates exhibited significantly less reduction in residual flexural strength for all cases of indented laminates as compared with 0° and 20°. This is due to high absorbed energy and more residual dent in laminates under 0° and 20° indentation loading. Significantly, CP laminates exhibited highest reduction in residual flexural strength in all loading planes.

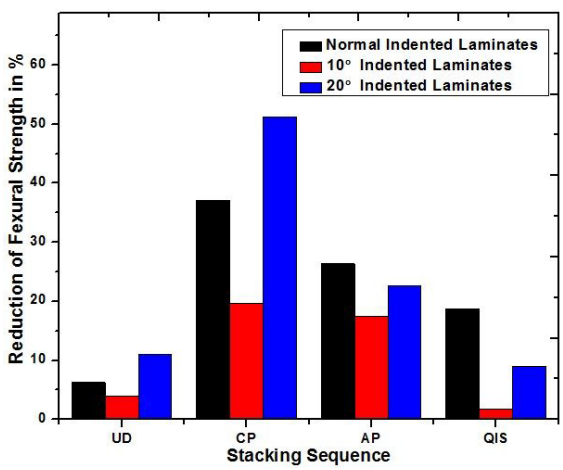

Figure 12. Reduction of residual flexural strength in indented laminates.

On the other hand, UD, QIS and AP laminates have lowest reduction of residual flexural strength under the indentation loading plane of 0°, 10° and 20° respectively. This reveals that the AP laminates exhibited better resistance to shear induced damages such as fiber/matrix interfacial debonding and delamination under 20° indentation loading plane.

4. Conclusions

In this study, the evolution of indentation induced damages and post-indented residual strength of different stacking sequence of glass/epoxy laminates were investigated under 0^o, 10^o and 20^o loading planes. The results concluded that the peak force was significantly reduced with increase the angle of loading plane due to the distribution of inclined indented force in to normal and shear forces. Further, the shear force is high at 20^o indentation plane which induced shear failure of fiber/matrix interfacial debonding and delamination for all cases of laminates. However, the mechanical results such as residual dent, linear stiffness and absorbed energy concluded that the QIS laminates having better indentation damage resistance under 0^o and 10^o loading planes, whereas the AP laminates performed well at 20^o. The degradation of structural integrity of the laminates was studied using normalized cumulative counts (NCC) and energy rate. Furthermore, the damage modes were discriminated using AE peak frequency range of 60 – 120 kHz, 130 – 180 kHz, 190 – 260 kHz and 270 – 320 kHz which are related to matrix cracking, delamination and fiber/matrix interfacial debonding and fiber failure respectively. The analysis of AE peak frequency concluded that the percentage of AE hits associated with shear failure has been reduced in AP as compared with QIS laminates under 20^o indentation plane. Further these results were correlated with different trends of sentry function. It can be concluded that the QIS and AP laminates have shown better resistance to indentation damage under 0^o and 10^o, and 20^o respectively. Therefore, AE is an effective method to characterize the damage initiation and propagation in laminated composites under different angles of indentation process.

5. References

1. Minak G, Abrate S, Ghelli D, Panciroli R, Zucchelli A. Low velocity impact on carbon/epoxy tubes subjected to torque - experimental results, analytical models and FEM analyses. Compos Struct. 2010;92:623-32.
2. Soutis C. Carbon fibre reinforced plastics in aircraft construction. Mater Sci Eng A. 2005;412(1-2):171-6.
3. Kumar CS, Arumugam V, Jack JK, Karthikeyan R, Jac Fredo AR. Experimental investigation on the effect of glass fiber orientation on impact damage resistance under cyclic indentation loading using AE monitoring. Nondestruct Test Eval. 2020;35(4):408-26.
4. Tanay TO, Gozluklu B, Gurses E, Coker D. Experimental and computational study of the damage process in CFRP composite beams under low-velocity impact. Compos, Part A Appl Sci Manuf. 2017;92:167-82.
5. Sohn MS, Hua XZ, Kimb JK, Walker L. Impact damage characterization of carbon fbre/epoxy composites with multi-layer reinforcement. Compos, Part B Eng. 2000;31:681-91.
6. Bull DJ, Spearing SM, Sinclair I. Investigation of the response to low velocity impact and quasi-static indentation loading of particle-toughened carbon-fiber composite materials. Compos, Part A Appl Sci Manuf. 2015;74:38-46.
7. Suresh Kumar C, Arumugam V, Santulli C. Characterization of indentation damage resistance of hybrid composite laminates using acoustic emission monitoring. Compos, Part B Eng. 2017;111:165-78.
8. Yuichiro A, Hiroshi S, Takashi I. Damage propagation in CFRP laminates subjected to low velocity impact and static indentation. Adv Compos Mater. 2007;16(1):45-61.
9. Jayababu A, Arumugam V, Rajesh B, Suresh Kumar C. Investigation of indentation damage resistance on normal and inclined plane of glass/epoxy composite laminates using acoustic emission monitoring. J Compos Mater. 2020;54(21):2953-64.
10. Akim D, Ramazan K. An experimental study on quasi-static indentation, low-velocity impact and damage behaviors of laminated composites at high temperatures. Polym Polymer Compos. 2021;29(9):S969-77.
11. Spronk SWF, Kersemans M, De Baerdemaeker JCA, Gilabert FA, Sevenois RDB, Garoz D, et al. Comparing damage from low-velocity impact and quasi-static indentation in automotive carbon/epoxy and glass/polyamide-6 laminates. Polym Test. 2018;65:231-41.
12. Zhong YN, Hu ZJ. The Use of quasi-static indentation testing to evaluate low-velocity impact resistance of ex situ toughened composite. Appl Mech Mater. 2014;697:35-40.
13. Wei H, Guan Z, Xing L, Liu D. Prediction of permanent indentation due to impact on laminated composites based on an elasto-plastic model incorporating fiber failure. Compos Struct. 2013;96:232-42.
14. Flores JEA, Li QM. Experimental study of the indentation of sandwich panels with carbon fibre-reinforced polymer face sheets and polymeric foam core. Compos, Part B Eng. 2011;42(5):1212-9.
15. Hachemane B, Zitoune R, Bezzazi B, Bouvet C. Sandwich composites impact and indentation behaviour study. Compos, Part B Eng. 2013;51:1-10.
16. Sang WK, Myung CC, In L, Eun HK, Il BK, Tae KH. Damage evaluation and strain monitoring of composite plate using metal-coated FBG sensors under quasi-static indentation. Compos, Part B Eng. 2014;66:36-45.
17. Caprino G, Spataro G, Del Luongo S. Low-velocity impact behavior of fibre glass-aluminum laminates. Compos, Part A Appl Sci Manuf. 2004;35:605-16.
18. Jac Fredo AR, Abilash RS, Femi R, Mythili A, Suresh Kumar C. Classification of damages in composite images using Zernike moments and support vector machines. Compos, Part B Eng. 2019;168:77-86.
19. Agastinose Ronickom JF, Retnakaran Sobhana A, Robert F, Sri Madhavan Raja N, Suresh Kumar C. Automated damage detection and characterization of polymer composite images using Tsallis-particle swarm optimization-based multilevel threshold and multifractals. Polym Compos. 2020;41(8):3194-207.
20. Shruthi K, Saravanakumar K, Arumugam V, Kumar CS. Effect of patch hybridization on indentation resistance and residual performance of patch repaired glass/epoxy laminates using acoustic emission monitoring. Nondestruct Test Eval. 2021;36(5):528-45.
21. Samuel R, Christophe B, Natthawat H. Failure analysis of CFRP laminates subjected to compression after impact: FE simulation using discrete interface elements. Compos, Part A Appl Sci Manuf. 2013;55:83-93.
22. Balan R, Arumugam V, Abdul Rauf K, Adhithya Plato Sidharth A, Santulli C. Estimation of residual flexural strength of unidirectional glass fiber reinforced plastic composite laminates under repeated impact load. J Compos Mater. 2015;49(6):713-22.
23. Santiuste C, Sanchez S, Barbero E. Residual flexural strength after low-velocity impact in glass/polyester composite beams. Compos Struct. 2010;92:25-30.
24. Yan-nan Z, Wei Z, Peng-fei Z. Quasi-static indentation damage and residual compressive failure analysis of carbon fiber composites using acoustic emission and micro-computed tomography. J Compos Mater. 2019;54(2):229-42.

25. Suresh Kumar C, Arumugam V, Sajith S, Dhakal HN, John R. Acoustic emission characterisation of failure modes in hemp/epoxy and glass/epoxy composite laminates. J Nondestr Eval. 2015;34(4):1-11.
26. Arumugam V, Suresh Kumar C, Santulli C, Sarasini F, Joseph Stanley A. A global method for the identification of failure modes in fiber glass using acoustic emission. J Test Eval. 2011;39(5):1-13.
27. Jayababu A, Arumugam V, Rajesh B, Suresh Kumar C. Damage characterization in glass/epoxy composite laminates under normal and oblique planes of cyclic indentation loading with AE monitoring. Mater Eval. 2021;79(1):61-77.
28. Suresh Kumar C, Pabitha P, Sengottuvelusamy R, Arumugam V, Srinivasan S. Optimization of acoustic emission parameters to discriminate failure modes in glass-epoxy composite laminates using pattern recognition. Struct Health Monit. 2018;18(4):1253-67.
29. Kumar CS, Saravanakumar K, Arumugam V. Characterization of failure mechanism in glass, carbon and their hybrid composite laminates in epoxy resin by acoustic emission monitoring. Nondestruct Test Eval. 2019;34(3):254-66.
30. Mei H, Sun Y, Zhang L, Wang H, Cheng L. Acoustic emission characterization of fracture toughness for fiber reinforced ceramic matrix composites. Mater Sci Eng. 2013;560:372-6.
31. Saravanakumar K, Suresh Kumar C, Arumugam V. Damage monitoring of glass/epoxy laminates with different interply fiber orientation using acoustic emission. Struct Health Monit. 2021;20(2):445-55.
32. Saravanakumar K, Farouk N, Suresh Kumar C, Arumugam V. Influence of milled glass fillers on mode-II fracture toughness of polymer composites. Mater Sci Technol. 2022;38(5):308-17.
33. Suresh Kumar C, Arumugam V, Sengottuvelusamy R, Srinivasan S, Dhakal HN. Failure strength prediction of glass/epoxy composite laminates from acoustic emission parameters using artificial neural network. Appl Acoust. 2017;115:32-41.
34. Maillet E, Godin N, Mili MR, Reynaud P, Lamon J, Fantozzi G. Analysis of Acoustic Emission energy release during static fatigue tests at intermediate temperatures on ceramic matrix composites: towards rupture time prediction. Compos Sci Technol. 2012;72(9):1001-7.
35. Mei H. Measurement and calculation of thermal residual stress in fiber reinforced ceramic matrix composites. Compos Sci Technol. 2008;68(15-16):3285-92.
36. Karthik MK, Kumar CS. A comprehensive review on damage characterization in polymer composite laminates using acoustic emission monitoring. Russ J Nondestr Test. 2022;58(8):705-21.
37. Kumar CS, Saravanakumar K, Prathap P, Prince M, Madhu S, Kumaran P. Effect of the reinforcement phase on indentation resistance and damage characterization of glass/epoxy laminates using acoustic emission monitoring. Adv Mater Sci Eng. 2021;5768730:1-11.
38. Amir Refahi O, Jalal Y. Characterization of residual strength in transversely loaded glass-polyester composites by acoustic emission and sentry function. Mater Today Proc. 2018;5(1):381-7.
39. Refahi Oskouei A, Zucchelli A, Ahmadi M, Minak G. An integrated approach based on acoustic emission and mechanical information to evaluate the delamination fracture toughness at mode I in composite laminate. Mater Des. 2011;32:1444-55.